Electronic Supplementary Information:

Vertically Aligned 2D SnS_2 Nanosheets with Strong Photon Capturing Capability for Efficient Photoelectrochemical Water Splitting

Guangbo Liu[a, c‡], Zhonghua Li[a‡], Tawfique Hasan[b‡], Xiaoshuang Chen[a], Wei Zheng[a], Wei Feng[a], Dechang Jia[d], Yu Zhou[d], PingAn Hu[a]*

[a]Key Laboratory of Micro-systems and Micro-structures Manufacturing of Ministry of Education, Harbin Institute of Technology, Harbin 150080, P. R. China.

[b]Cambridge Graphene Centre, University of Cambridge, Cambridge, CB3 0FA, UK

[c]School of Chemistry and Chemical Engineering, Harbin Institute of Technology, Harbin, 150001, P. R. China.

[d]Institute for Advanced Ceramics, Harbin Institute of Technology, Harbin 150001, China

[*]Corresponding author. Email: hupa@hit.edu.cn

‡ These authors contributed equally to this work.

Experimental Details

Synthesis of Vertical 2D SnS_2 Nanosheets. Vertically aligned 2D SnS_2 nanosheets

grown on FTO and CC substrates were synthesized by CVD method in a two-temperature zone tube furnace. In a typical growth procedure, 100 mg $SnCl_4 \cdot 5H_2O$ powder was loaded in an alumina boat, was placed at the center of the downstream heating zone. A series of growth substrates (FTO and CC) were placed downstream to the $SnCl_4 \cdot 5H_2O$ powder. The distance of the $SnCl_4 \bullet 5H_2O$ alumina boat and the substrates were 3, 8 and 11 cm, respectively. 200 mg S powder was placed in another alumina boat at the upstream heating zone. Before the start of the growth, the furnace chamber was flushed with 1200 sccm high purity Ar gas for ~20 min to decrease the oxygen content in the chamber. Next, the center of the downstream heating zone was heated to 450°C from room temperature at a ramp rate of 10℃. At the same time, the temperature of the S powder at the upstream heating zone was set to 250℃. The temperature in the downstream heating zone was kept at 450°C for 5 min for the SnS_2 growth under a mixture carrier gas of H_2 (15 sccm) and Ar (45 sccm). After the growth, the furnace was naturally cooled down to room temperature and vertically oriented 2D SnS_2 nanosheets on FTO and CC substrates were obtained.

Characterizations. The crystallographic information for the samples was collected using a Philips Panalytical X'Pert Pro multipurpose diffractometer with Cu-Kα X-ray radiation (λ= 1.5418 Å). The morphologies of the samples were examined using a Hitachi SU8000 field-emission scanning electron microscope (FE-SEM) with a 20 kV accelerating voltage. The detailed microstructure, growth orientations and composition of the as-grown 2D SnS_2 nanosheets were carried out by a Tecnai-G2 F30 transmission electron microscop (TEM) attached with an energy dispersive X-ray

spectroscopy (EDS) system, operating at 300 kV. The temperature gradient in the furnace was detected by using a TES-1310 digital thermometer equipped with a WRNK-81530 thermocouple (TES Electrical Electronic Corp., Taipei). The UV-Visible extinction spectra were recorded on a Hitachi U-4100 UV-Vis-NIR spectrophotometer.

Photoelectrochemical Measurements. Prior to the measurements, the 2D SnS_2 nanosheets grown on FTO and CC substrates were first fabricated into photoanodes by soldering a Cu mesh onto the bare part of the substrates. The area of the growth substrates was ~ 1 cm × 1 cm, and the loading amount of the 2D SnS_2 nanosheets was in the range of 0.25-0.30 mg/cm^2 (D_{ss}=11cm, temp=337±1℃). The deposition amount was estimated by weighing the difference in substrate's weight before and after the growth using an analytical balance with 0.01 mg resolution (XS105 DualRange, Mettler Toledo). For the preparation of parallel photoanode counterparts, vertically aligned 2D SnS_2 nanosheets grown on FTO/CC substrates were firstly separated from their growth substrates in ethanol-water solution by using ultrasonic treatment. After that, the 2D SnS_2 nanosheets products were obtained in the ethanol-water solution. Then, the parallel 2D SnS_2 nanosheets photoanodes were obtained as the above-obtained solution was deposited onto a 1 cm × 1 cm FTO substrate and acquired a loading amount in the range of 0.25-0.30 mg/cm^2 after drying process.

The photoelectrochemical properties were investigated in a conventional three-electrode system on an electrochemical workstation (CHI660D, CH Instruments), with single-compartment quartz cell, a Pt foil counter electrode and an Ag/AgCl

reference electrode. The fabricated photoanodes were used as the working electrode. Na_2SO_4 solution (0.5 M, pH=7.58) was used as electrolyte after saturation with N_2 gas for 30 min. The measured Ag/AgCl reference electrode potentials were converted to V vs. reversible hydrogen electrode (RHE) by using the formula $E_{RHE} = E_{Ag/AgCl} + 0.0591pH + 0.1976$ V. The photocurrent was measured by linear sweep voltammetry in the range of 0.2-1.4 V vs. RHE at a scan rate of 10 mV/s. Visible-light irradiation was achieved by a 500 W Xe lamp (CHF-XM500, Trusttech Co., Ltd.) fitted with an AM 1.5 G filter. The light intensity was tuned to one Sun (100 mW/cm^2). The time-dependent current change curves were measured at the bias potential of 1.2 V vs. RHE under the same 500 W Xe lamp irradiation. Electrochemical impedance spectroscopy (EIS) was carried out at a bias potential of 1.2 V vs. RHE with a frequency range of 100 kHz-100 mHz using the same lamp. The measured spectra were fitted to the corresponding equivalent circuit model by using the program ZView (Scribner Associates Inc.). The IPCE value was measured under monochromatic light illumination by the 500 W Xe lamp through a monochromator (Omni λ-3007, Zolix Instruments Co., Ltd.). The monochromator was incremented through the spectral range (360-660 nm) to generate a photocurrent action spectrum with a sampling interval of 20 nm. The light intensity was measured using a thermal power sensor (S310C, Thorlabs) equipped with a readout power meter (PM100D, Thorlabs). Conductivity characterizations of bare FTO and different $SnS_2 \perp$FTO photoelectrodes were performed by using a semiconductor characterization system (Keithley 4200 SCS) with a Lakeshore probe station.

Supplementary Figures

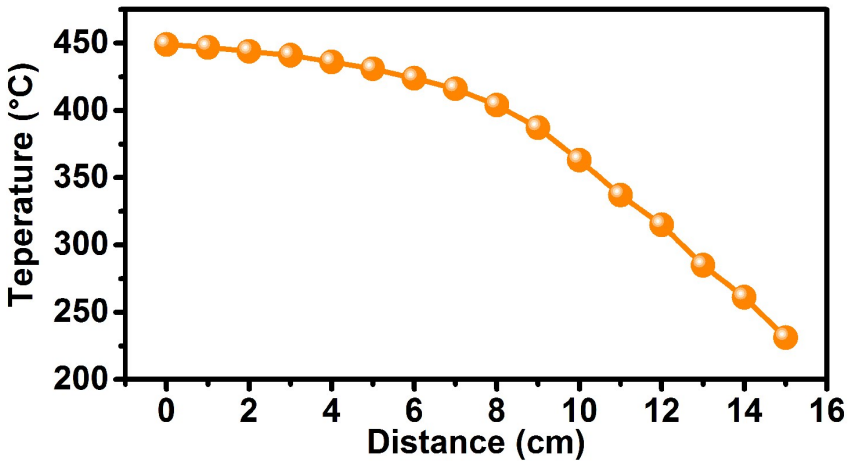

Figure S1. The temperature distribution in the furnace.

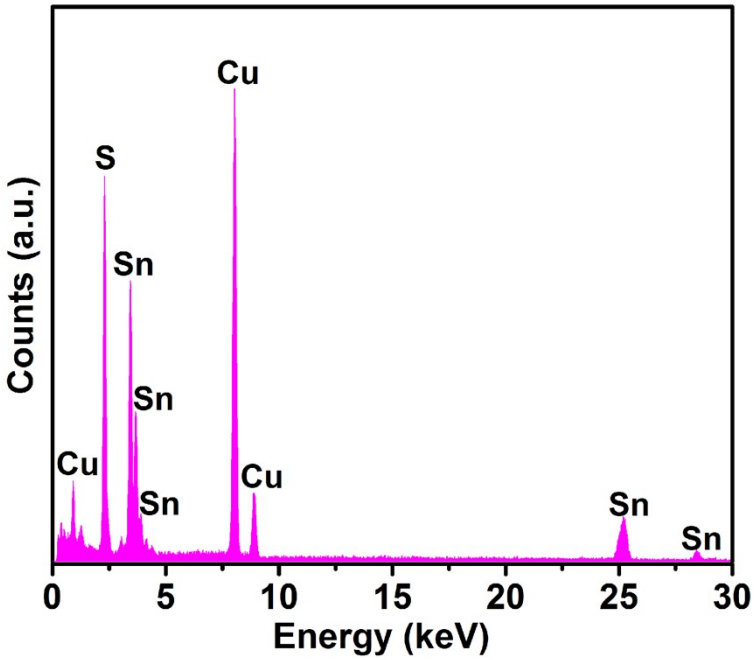

Figure S2. EDS spectrum of vertically aligned SnS_2 nanosheets. EDS spectrum of the as-grown vertically aligned SnS_2 nanosheets confirming the elemental ratio of Sn and S is ~1:2.

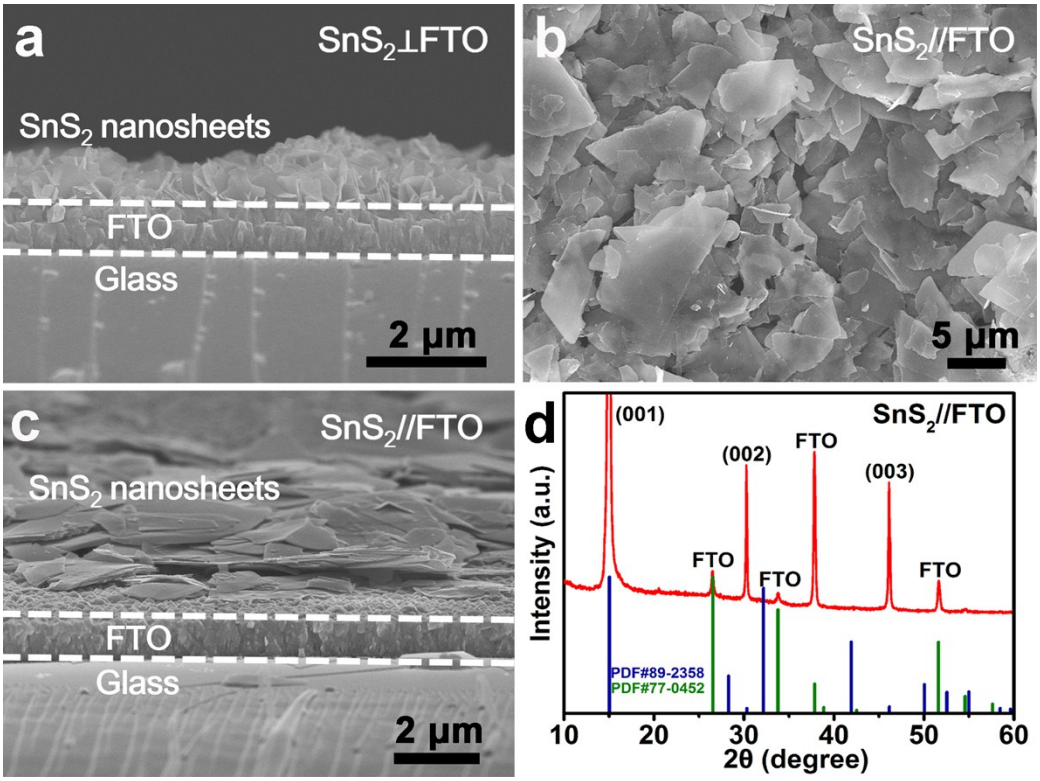

Figure S3. SEM characterizations of $SnS_2 \perp$FTO and SnS_2//FTO photoelectrodes. (a) Cross-sectional SEM image of $SnS_2 \perp$FTO photoelectrode. (b) SEM image of SnS_2//FTO photoelectrode. (c) Cross-sectional SEM image of SnS_2//FTO photoelectrode. (d) XRD pattern of SnS_2//FTO photoelectrode. The XRD pattern of SnS_2//FTO photoelectrode reveals three diffraction peaks assigned to the (001), (002) and (003) facets for the hexagonal SnS_2, indicating the [001] basal orientation is highly preferred on FTO substrate, which is notably different from that of the $SnS_2 \perp$FTO and $SnS_2 \perp$CC photoelectrodes (main text Fig. 3a).

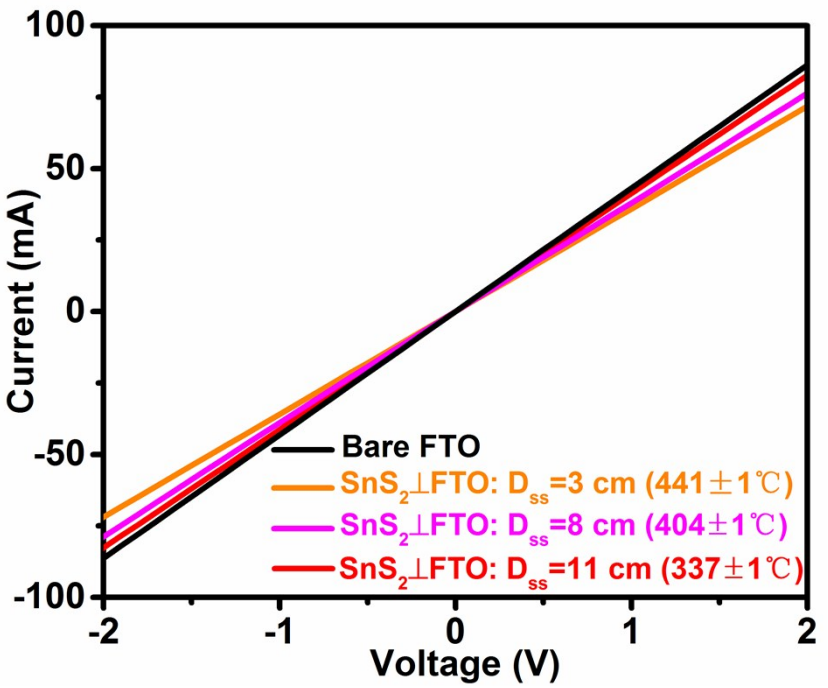

Figure S4. Comparison test of the conductivity of bare FTO and different SnS_2⊥FTO photoelectrodes. The current-voltage curves show little or no difference between the as-grown SnS_2⊥FTO photoelectrodes and bare FTO, implying our growth strategy makes no change to the conductivity of FTO after grown catalytic material, which is essential for the as-grown SnS_2⊥FTO photoelectrodes whether or not can be used in high performance PEC water splitting.

Supplementary Table S1. Comparison of PEC performance of the vertically aligned 2D SnS_2 nanosheets with other 2D-baesed photoelectrode materials.

Photoelectrode materials	Preparation method	Electrolyte	Photocurrent density (mA/cm^2)	IPCE (%)	Reference
Zr-β-In_2S_3 nanoflake	hydrothermal	0.5 M NaOH	1.1 mA/cm^2 at 1.3V vs RHE	2.5% at 300 nm	1
β-In_2S_3 nanoflake	hydrothermal	0.5 M NaOH	0.37 mA/cm^2 at 0.7 V vs Ag/AgCl	-	2
CdS-WS_2 nanosheets	liquid exfoliation	0.05 M Na_2S	0.35 mA/cm^2 at 0.1 V vs SCE	-	3
CdS-MoS_2 nanosheets	liquid exfoliation	0.05 M Na_2S	0.28 mA/cm^2 at 0.1 V vs SCE	-	4
WSe_2 thin films	liquid exfoliation	1 M H_2SO_4	1.0 mA/cm^2 at 0 V vs RHE	20% at 400 nm	5
ZnS thin films	pulsed laser deposition	0.24 M Na_2SO_3	1.6 mA/cm^2 at 1.0 V vs Ag/AgCl	8% at 200 nm	6
Au-MoS_2 nanosheets	hydrothermal	0.1 KH_2PO_4	0.79 mA/cm^2 at 0.8 V vs Ag/AgCl	-	7
MoS_2 nanosheets	hydrothermal	0.1 M KH_2PO_4	0.26 mA/cm^2 at 1.0 V vs Ag/AgCl	-	8
SnS_2 single-layers	liquid exfoliation	0.5 M Na_2SO_4	2.75 mA/cm^2 at 1.0 V vs Ag/AgCl	38.7% at 420 nm	9
SnS_2 nanosheets	solvothermal	0.5 M Na_2SO_4	0.017 mA/cm^2 at 0.8 V vs SCE	-	10
parallel SnS2//FTO	chemical vapor deposition	0.5 M Na_2SO_4	0.91 mA/cm^2 at 1.4 V vs. RHE	18.68% at 360 nm	This work
vertically aligned SnS_2⊥CC			1.92 mA/cm^2 at 1.4 V vs. RHE	40.57% at 360 nm	
vertically aligned SnS_2⊥FTO			1.73 mA/cm^2 at 1.4 V vs. RHE	36.76% at 360 nm	

Supplementary References

1 L. Wang, L. Xia, Y. Wu and Y. Tian, *ACS Sustain Chem Eng*, 2016, **4**, 2606-2614.

2 Y. Tian, L. Wang, H. Tang and W. Zhou, *J Mater Chem A*, 2015, **3**, 11294-11301.

3 M. Zirak, M. Zhao, O. Moradlou, M. Samadi, N. Sarikhani, Q. Wang, H. L. Zhang and A. Z. Moshfegh, *Sol Energ Mater Sol C*, 2015, **141**, 260-269.

4 M. Zirak, M. Ebrahimi, M. Zhao, O. Moradlou, M. Samadi, A. Bayat, H. L. Zhang

and A. Z. Moshfegh, *RSC Advances*, 2016, **6**, 16711-16719.

5 X. Yu, M. S. Prevot, N. Guijarro and K. Sivula, *Nat Commun*, 2015, **6**, 7596.

6 F. Kurnia, Y. H. Ng, R. Amal, N. Valanoor and J. N. Hart, *Sol Energ Mater Sol C*, 2016, **153**, 179-185.

7 Z. Yin, B. Chen, M. Bosman, X. Cao, J. Chen, B. Zheng and H. Zhang, *Small*, 2014, **10**, 3537-3543.

8 X. Xu, J. Hu, Z. Yin and C. Xu, *Acs Appl Mater Interfaces*, 2014, **6**, 5983-5987.

9 Y. Sun, H. Cheng, S. Gao, Z. Sun, Q. Liu, Q. Liu, F. Lei, T. Yao, J. He, S. Wei and Y. Xie, *Angew Chem Int Ed*, 2012, **51**, 8727-8731.

10 J. Yu, C. Y. Xu, F. X. Ma, S. P. Hu, Y. W. Zhang and L. Zhen, *Acs Appl Mater Interfaces*, 2014, **6**, 22370-22377.